Computation of Confined Turbulent Coaxial Jet Flows

M. Nallasamy*
Sverdrup Technology, Inc., Cleveland, Ohio

Confined turbulent coaxial jet flows are investigated numerically, employing the k-ϵ turbulence model. The geometrical arrangement corresponds to the experimental study of Owen. The shape, size, and location of the recirculation zones predicted by the present numerical model are in good agreement with the experiment. The processes leading to the observed flow pattern are explained. It is shown that the shape, size, and location of the recirculation zones are controlled by the central jet tip geometry and the velocity ratio of the jets.

Nomenclature

d = diameter of the central jet
D_0 = diameter of the annular jet
D_e = diameter of the expansion chamber (Fig. 1)
DR = diameter ratio of the jets, D_0/d
ER = expansion ratio, D_e/D_0
k = turbulence kinetic energy
S_ϕ = source term for ϕ, Eq. (1)
U_a = velocity of the annular jet
U_p = velocity of the central jet
V = velocity vector
α = velocity ratio of the jets, U_a/U_p
Γ_ϕ = diffusion coefficient of ϕ
ϵ = dissipation rate of turbulence energy
ρ = fluid density
ϕ = fluctuating scalar quantity

Subscripts

in = at the inlet section
ϕ = of the fluctuating scalar quantity ϕ

I. Introduction

THE everpresent demand for high-power-density engines for spacecraft has resulted in engine designs that require the combustion system to operate at high pressure levels, higher fuel/oxidizer velocities, and increased outlet temperatures. The new design methodologies are greatly assisted by noninvasive laser Doppler anemometer (LDA) measurements in model combustors and advancement in combustion modeling resulting from the improvements in the numerics and computer memory and speed. One of the flow configurations often employed in modern combustors (for example, the Space Shuttle) is that of coaxial jet flow. In this configuration, when the ratio of the velocity of the annular jet to that of the central jet is high, a large central toroidal recirculation zone is formed in addition to the corner recirculation zone (Fig. 1). These are the most important flow regions in any combustor flowfield. Most of the combustion occurs in and near the recirculation zones. Maldistribution of high temperatures occurs in the practical combustor flowfield when the unburned fuel escapes the recirculation zones and travels downstream. To correct maldistribution of high temperatures, details of the flowfield and the means of controlling it should be known. Numerical simulation of the flow is now increasingly employed to define and understand the combustor flowfield.[1-4]

Practical combustor flowfields are turbulent, three-dimensional, multiphase, chemically reacting, and radiating. Numerical simulations consider the complex processes through appropriate simplified models.[5,6] The turbulence in the flow is taken care of by introducing closure models. The two-equation, k-ϵ model is often employed. In the currently available numerical simulation methods, models for chemical species calculation and radiation are particularly weak and need improvement.[2] A combination of idealized experiments, predictive methods, and developments is helpful in making progress in numerical modeling. With this in mind, detailed experiments on two-dimensional axisymmetric flow have been carried out and reported in the literature for use in validating the mathematical models.

The coaxial jet flow is a complex one, consisting of large recirculation zones whose occurrence depends on parameters such as the ratio of the velocities of the jets, ratio of the diameters of the jets, expansion ratio, inlet swirl, etc. Figure 1 shows the typical recirculation zones: 1) a corner recirculation zone present in most coaxial jet flow geometries and operating conditions with no inlet swirl and 2) a central toroidal recirculation zone whose formation in nonswirling flows depends mainly on the geometry and velocity ratio. The numerical methods that model the coaxial jet flow need to predict these flow regions reasonably accurately if the models are to be useful to the designer. The availability of reliable data for comparison with the calculation is a prerequisite for testing a numerical model. In an effort to provide such data and also to understand the nature of the flow in a coaxial jet flow configuration of interest to a combustor designer, Owen[7] carried out detailed turbulence measurements using LDA.

Novick et al.[8], Syed and Sturgess,[9] and Sturgess et al.[10] predicted the confined coaxial jet flow corresponding to the experimental conditions of Owen[7] by employing the k-ϵ turbulence model. However, the predicted shape, size, and location of the recirculation zones differed significantly from the experiment. The reasons for the discrepancies were not clear. A detailed examination of the k-ϵ model predictions for similar flows by the present author indicated that the turbulence model cannot account for all the discrepancies. The present investigation was undertaken to study the characteristics of recirculation zones in coaxial jet flows in general and, in particular, to examine and improve the predictions corresponding to Owen's experiment.

Received Nov. 13, 1985; presented as Paper 86-0128 at the AIAA 24th Aerospace Sciences Meeting, Reno, NV, Jan. 6-8 1986; revision received Nov. 24, 1986.

*Senior Research Engineer. Member AIAA.

II. The Problem

In coaxial jet flows with a high velocity ratio, a central toroidal recirculation zone is formed due to the imbalance of the mass flow between the central and annular jets. The sudden expansion of the annular jet results in a severe (depending on the velocity ratio) adverse pressure gradient. When this pressure gradient is too strong for the low-momentum central jet, a central toroidal recirculation zone results in addition to the corner recirculation zone (Fig. 1). The size and locations of these zones are important in combustors.

The factors that influence the size, shape, and location of the recirculation zones in a coaxial jet flow are the velocity ratio of the jets, diameter ratio of the jets, details of the central jet tip geometry, expansion ratio, and the properties of the central and annular jet fluids. For the given fluids and geometrical configuration, the velocity ratio influences the recirculation zones. The aim of the present investigation is twofold: 1) to predict the coaxial jet flow corresponding to the experimental configuration of Owen[7] and 2) to investigate the sensitivity of the recirculation zones to the details of the central jet tip geometry and the velocity ratio of the jets.

Owen's experimental configuration (Fig. 2) consisted of a 2.5 in. (6.35 cm) central jet surrounded by a 3.5 in. (8.89 cm) annular jet. The jets discharge into a 5 in. (12.7 cm) diameter chamber 48 in. (121.9 cm) long. The outer and inner peak velocities were 96.0 and 8.0 ft/s (29.26 and 2.44 m/s), corresponding to Reynolds numbers based on respective diameters of 1.5 and 0.08×10^5. No measured inflow profiles were reported.

III. The Numerical Method

Calculation of the confined coaxial jet flowfield with large regions of recirculation requires the solution of the spatially elliptic form of the governing equations. The equations representing the conservation of mass, momentum, turbulence kinetic energy, and its rate of dissipation are represented in the general form,[11]

$$\mathrm{div}(\rho V\phi) = \mathrm{div}(\Gamma_\phi \mathrm{grad}\phi) + \dot{S}_\phi \tag{1}$$

where ϕ is a fluctuating scalar quantity—a velocity component, turbulence energy, or its dissipation rate. The equations are discretized by employing the finite-volume method of discretization and the resulting equations are solved numerically. The inlet section was located at a distance 0.75 D_0 upstream of the expansion plane (Fig. 1). A fully developed flow was specified at the inlet. The inlet profiles for k and ϵ were specified in the usual manner,[12]

$$k_{\text{in}} = 0.003\ U_{\text{in}}^2 \tag{2}$$

$$\epsilon_{\text{in}} = 0.09\ k^{1.5}/(0.03\ D/2) \tag{3}$$

The computational grid used for all the computations consisted of 40×40 nonuniformly distributed nodes, with a high gridline concentration in the separated shear layer and near the walls. The grid extended to an axial distance of 11.25 D_0. Tests showed that this nonuniform grid produced a nearly mesh-independent solution (with little change in the size of the recirculation zones). All the computations were performed by means of the PHOENICS computer program of Spalding.[13] One of the very useful concepts adopted in the program is that of "porosity," used to modify the regular grid cells. Irregular geometry and blockages in the flowfield can be conveniently represented using the grid porosity. This is done by specifying a set of factors that will multiply the areas/volumes associated with the grid that has been nominally established. In the present computation, partially or fully blocked grid cells were represented by using porosity.

IV. Discussion of Results

First, we will describe the predictions of the flowfield corresponding to the experimental conditions of Owen.[7] Then, we will discuss the sensitivity of the recirculating zones to different controlling parameters.

Predictions of the Flowfield for Owen's Experimental Configurations

The coaxial jet flow patterns corresponding to Owen's experimental configuration are shown in Fig. 3. The flow patterns predicted by Novick et al.[8] and Sturgess et al.[10] are shown here in Figs. 3a and 3b, respectively, for comparison. In these predictions, the shape, size, and location of the recirculation zones differ significantly from the experiment (Fig. 3d). The flow pattern predicted by the present numerical model (Fig. 3c) shows good agreement with the flow pattern obtained in the experiment. The part of the present numerical model/code responsible for the improved prediction is discussed below.

Recognition of the fact that the central jet tip geometry is the critical element and should be modeled accurately is responsible for the present improved prediction. Use of the grid porosity concept in PHOENICS code (Sec. III) to represent irregular geometry and blockages in the flowfield facilitates an accurate modeling of the central jet tip geometry. In the present prediction (Fig. 3c), the central jet tip is modeled exactly as in the experimental setup (Fig. 2). That is, the central jet tip projects into the expansion chamber and is chamfered. This accurate modeling of the jet tip simulates the experimentally observed flow pattern. (See also the discussion corresponding to Fig. 9c).

The flow predictions in Refs. 8 and 10 were obtained using codes based on the TEACH code described in Ref. 14. The TEACH and PHOENICS codes employ the same form of time-averaged equations that govern the flow and k-ϵ turbulence models. Both codes use a finite-volume/area method of discretization. The PHOENICS code employs an upwind difference scheme and the TEACH-based codes a hybrid,

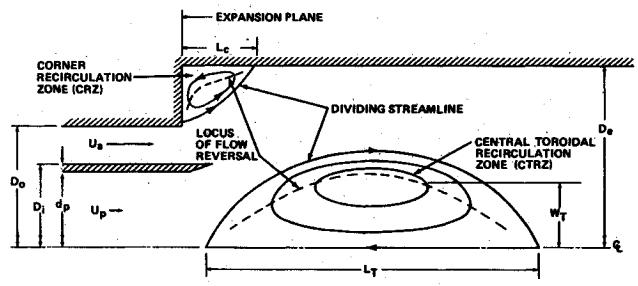

Fig. 1 Definition sketch.

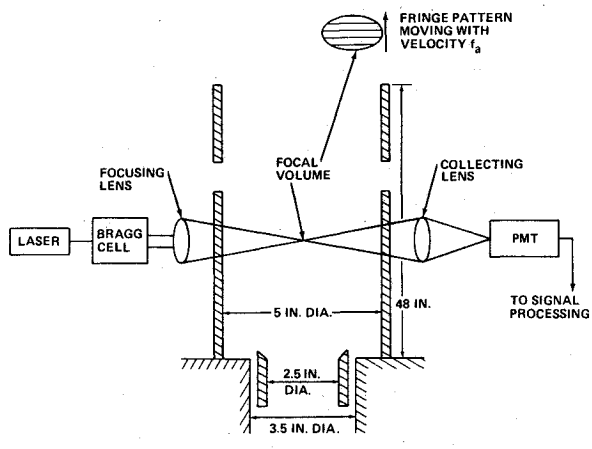

Fig. 2 Schematic of the coaxial jet flow experiment of Owen.[7]

central-upwind scheme. A comparison of the predictions of the two codes on a model problem—flow in a pipe expansion—was made by Nallasamy and Chen.[15] They found that, although the details of the turbulence energy distribution and the velocity profile near the wall produced by the two codes differed slightly, the predicted flow patterns were similar. In other words, the present improved prediction of the coaxial jet flow is not brought about by the nature of the formulation or the solution algorithm of the PHOENICS code, but by the accurate modeling of the central jet tip geometry. In what follows, a physical explanation of the processes leading to the formation of recirculation zones of observed sizes is given and then detailed comparisons of the predictions with measurements are presented.

For the velocity ratio (=12) considered here, the growth of the mixing layers emanating from the tips of the inner and outer jet walls is essentially controlled by the outer jet. When the inner jet wall ends at the expansion plane, the (virtual) origins of both inner and outer mixing layers are at the expansion plane. Then, the spread of the two mixing layers is about the same, resulting in the same value for the lengths of the corner and central recirculation zones (Fig. 4). This is the result observed in earlier predictions of the flow,[8, 10] as well as in the present study of this configuration (see Fig. 9c below). However, for the configuration of the experiment, the origin of the inner mixing layer is shifted downstream to 0_2, while the origin of the outer mixing layer remains unchanged. The spreading rate of the inner mixing layer is about the same as before (except for the modification due to the interactions of the two mixing layers). This results in a longer central recirculation zone, as shown in Fig. 4. The length of the corner recirculation zone is reduced because of the stabilizing effect of the extending central jet wall. This is similar to the stabilizing effect of the extending central jet wall. This is similar to the stabilizing effect in the asymmetric channel expansion—flow over a backward-facing step, where the length of the recirculation zone is small compared to the symmetric channel expansion.[12] These two processes result in the observed shape, size, and location of the recirculation zones.

The centerline mean axial velocities obtained in the present prediction and experiment are shown in Fig. 5. The agreement betweeen the two is good up to a distance of 2.25 D_0. Beyond this, the predicted value is smaller than the measured one. This is due to the slow development of the flow beyond the reattachment of the dividing streamline on the centerline. The slow redevelopment of the flow has been observed in most k-ϵ model predictions of recirculating flows.[16,17] The observed redevelopment is due to the inability of the k-ϵ model to represent this region correctly where the flow is changing from a separated to reattached one. It is not characteristic of either a boundary or a free-shear layer. The axial turbulence intensity on the centerline is shown in Fig. 6. The agreement with the measurements is very good up to an axial distance of 1.75 D_0. Beyond this, the turbulence intensity falls more quickly than it did in the experiment. This appears to be due to the incorrect representation of the redevelopment of the flow in the model. However, the general shape of the profile is correctly predicted.

Figure 7 shows the radial profiles of the mean axial velocity at two axial locations, $X=0.36$ and 1.43 D_0. The predicted velocity profiles are in reasonably good agreement with the measurements. The maximum discrepancies observed are in the region of maximum shear. The mean radial velocity profiles at the two downstream sections are shown in Fig. 8. At the section near the jet exit ($X=0.36$ D_0), the computation shows a negative radial velocity region near the expansion chamber wall. No experimental points have been shown in this region (the line drawn through the experimental points shows no negative velocities[7]). The negative radial velocity observed in the prediction is to be expected, due to the corner recirculation zone, and no velocity components were measured in this zone. At the downstream section

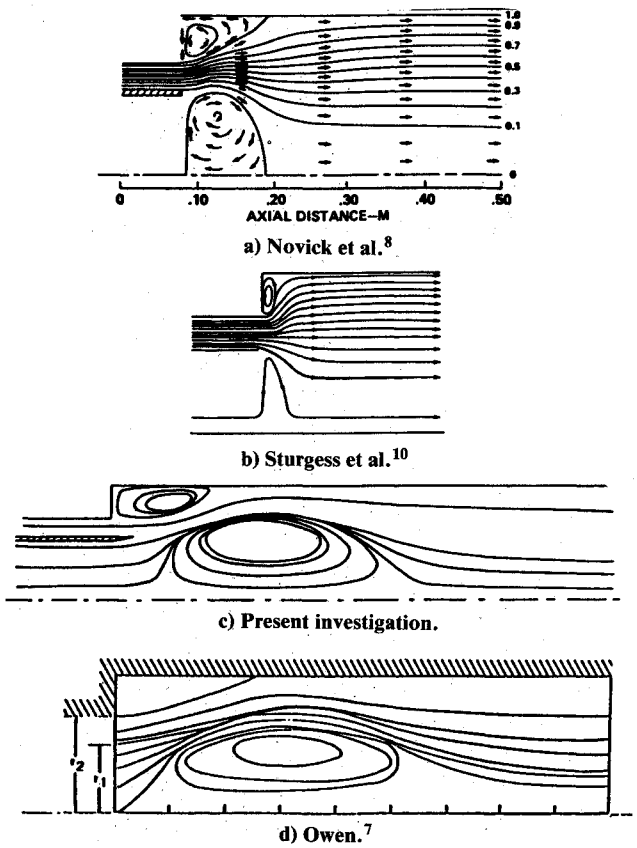

Fig. 3 Predicted and measured flow patterns. a) Novick et al.[8] b) Sturgess et al.[10] c) Present investigation. d) Owen.[7]

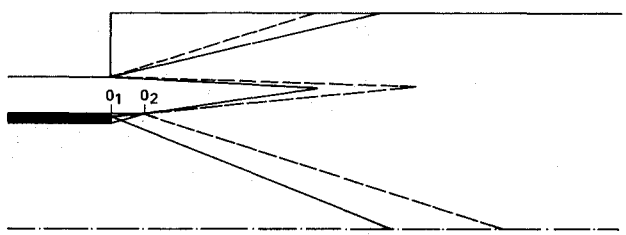

Fig. 4 Growth of mixing layers (– – – experimental configuration, — predictions of Refs. 8–10).

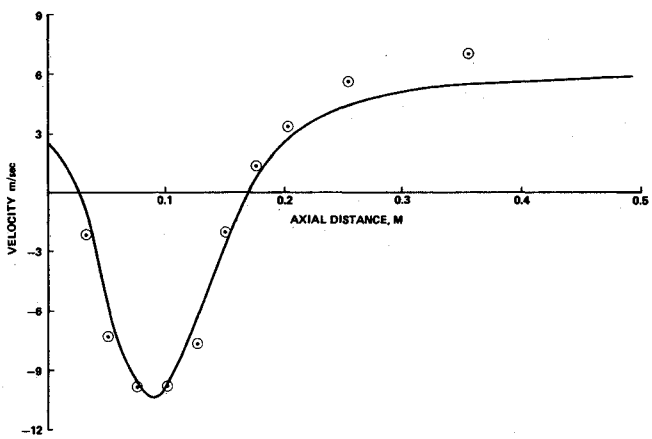

Fig. 5 Axial mean velocity along the centerline (— prediction, ⊙ measurement[7]).

($X=1.43\ D_0$), the predicted velocities are in reasonable agreement with the measurements. The maximum discrepancy occurs in the wake region of the jet wall at both axial stations. This is in accordance with the observation of Pope and Whitelaw.[18]

The detailed comparisons of axial and radial mean velocities, turbulence intensities, and recirculation zones show that the present computations produce the coaxial jet flowfield reasonably accurately. The sensitivity of the recirculation zones to the central jet exit geometry is presented below.

Effects of Central Jet Exit Configuration

The central jet exit geometrical configuration is designed according to the requirements of flame length (recirculation zone length) and stability. Five different configurations of the central jet exit geometry and the predicted recirculation zone boundaries for each case are shown in Fig. 9. The locii of the flow reversals ($\bar{U}=0$) have been plotted for the corner and central recirculation zones. The longitudinal extent of these regions is in accordance with the expectations based on Fig. 4. Thus, the effects of central jet exit geometry are qualitatively well predicted in the present computations (no experimental data are available for direct comparison). A configuration similar to that shown in Fig. 9a is employed in the Space Shuttle main engine injector elements to introduce fuel and oxidizer into the preburners and the main combustion chamber. In this case, the central recirculation zone starts well before the expansion plane. In Fig. 9b, the blunted edge of the central jet wall pushes the central recirculation zone a little downstream (due to a thicker wake region) and increases the length of the corner recirculation zone. The configuration studied by Novick et al.[8] and Sturgess et al.[10] is shown in Fig. 9c. In this case, since the two mixing layers grow from the same section (expansion plane), the shape of the central recirculation zone is quite different from those of Figs. 9a and 9b. The lengths of the two recirculation zones [corner recirculation (CRZ) and central toroidal (CTRZ)] are almost the same, as observed in the previous investigations. Figure 9d shows the recirculation zones for the case where the central pipe wall extends beyond the expansion plane. This produces a location, shape, and size of the recirculation zones very close to the experimentally observed ones. However, only when the pipe edge is

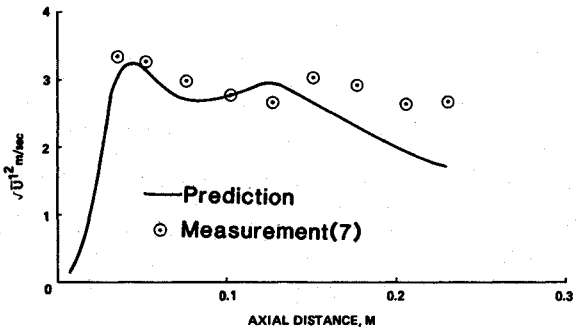

Fig. 6 Axial turbulence intensity on the centerline.

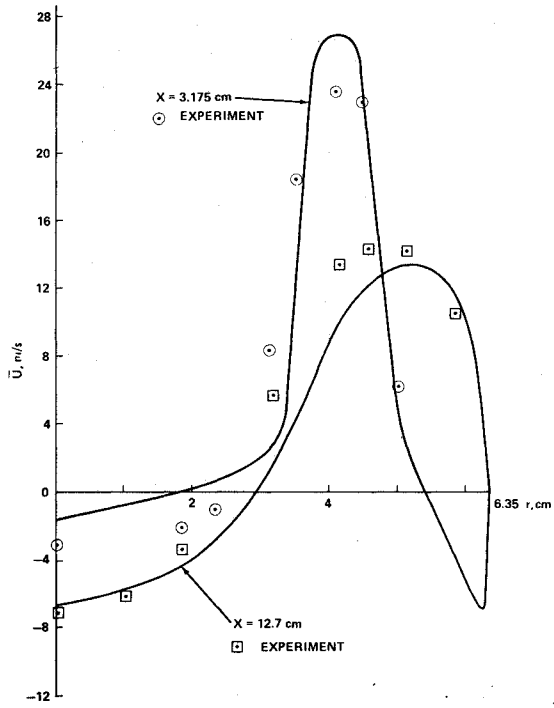

Fig. 7 Mean axial velocity profiles.

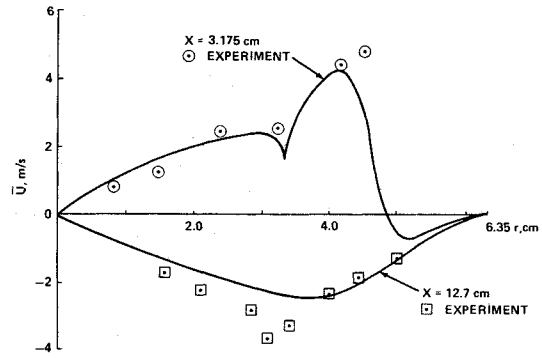

Fig. 8 Mean radial velocity profiles.

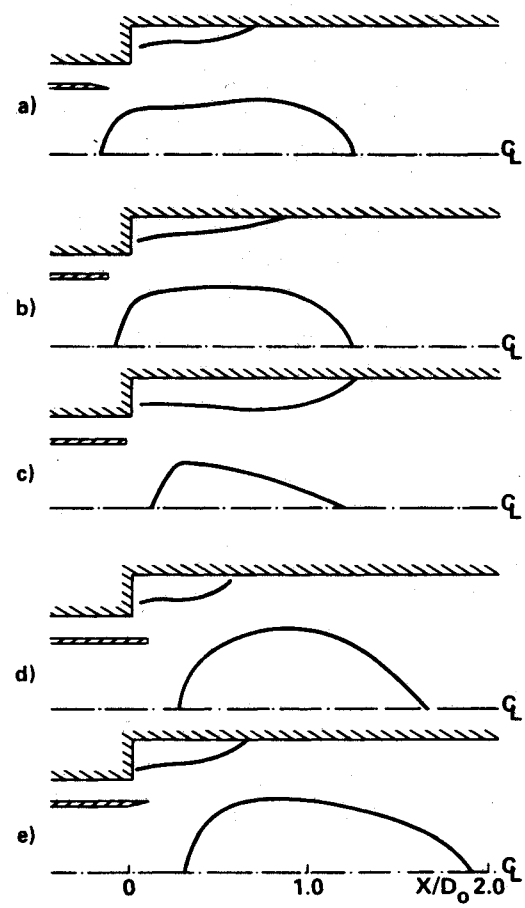

Fig. 9 Variations of locii of flow reversals with central jet exit configurations.

chamfered, as in the experimental configuration (Fig. 9e), will the size, shape, and location of CRZ and CTRZ be similar to those of the measurements (see also Fig. 3c). Thus, it is shown that the sensitivity of the recirculation zones to the central jet exit geometry can be correctly predicted by the numerical solution. This can aid the designer in selecting the configuration of the central jet exit geometry.

The observed changes in the characteristics of the recirculation zones with the pipe wall exit geometry should result in significant changes in wall static pressure beyond the expansion plane. Figure 10 shows the wall static pressure variation corresponding to Figs. 9a, 9c, and 9e. Only these cases are shown for clarity. The pressure recovery is faster for the configuration in Fig. 9a where the length of the CRZ is small and the CTRZ starts well before the expansion plane. For the case in Fig. 9c, the recovery is much slower because the CRZ is longer. For the experimental configuration shown in Fig. 9e, the wall static pressure variation is quite different from those in Figs. 9a and 9c. The initial recovery is faster since the length of CRZ is small, as in Fig. 9a. But the pressure coefficient drops again due to the growth of the width of the CTRZ even beyond the extent of the CRZ. The wall static pressure in the expansion chamber is thus very sensitive to the central jet exit geometry.

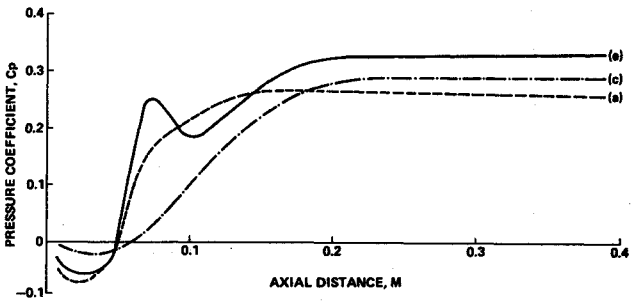

Fig. 10 Computed wall static pressure (—configuration of Fig. 9a, – · – configuration of Fig. 9c, – – – configuration of Fig. 9e).

Effect of Velocity Ratio

It has been shown that for the experimental conditions of Owen,[7] the flowfield can be predicted reasonably well. For the same geometrical configuration, the effect of the velocity ratio on the recirculation zones is examined. The central toroidal recirculation boundaries for four velocity ratios, namely 12, 9, 6, and 3, are shown in Fig. 11. No CTRZ is formed for a velocity ratio of 2 or 1. With the reduction in velocity ratio from 12 to 6, the distance of the CTRZ from the expansion plane increases, i.e., the separation bubble moves downstream gradually. However, for a velocity ratio of 3, the CTRZ is pushed far downstream.

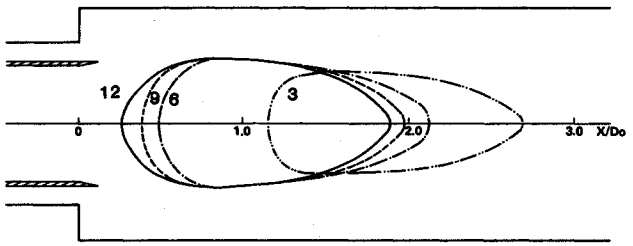

Fig. 11 Effect of velocity ratio on the central toroidal recirculation zone (—$\alpha=12$, – – – $\alpha=9$, – · – $\alpha=6$, – ·· – $\alpha=3$).

The observed behavior of the CTRZ with the velocity ratio may be understood from the mixing layer characteristics. Figure 12 shows the growth rate of the thickness of a two-stream mixing layer plotted against the velocity difference parameter λ (adopted from Brown and Roshko[19]). If U_1 and U_2 are the velocities of the two streams, then λ is defined as $\lambda=(U_1-U_2)/U_1+U_2)$. As we decrease the velocity ratio from 12 to 6, the growth rate of the mixing layer decreases gradually. The smaller the growth rate the farther the separation bubble moves from the expansion plane. For a velocity ratio of 3, λ becomes 0.5 and the growth rate differs significantly from that for $\alpha=6$. This means slow development of the mixing layer, which is reflected in the movement of the CTRZ far downstream for $\alpha=3$. For a velocity ratio of 2, the growth rate is small and the adverse pressure gradient is not strong enough to produce a CTRZ. It is interesting to note that the length of the CTRZ does not change significantly when the velocity ratio increases from 3 to 12.

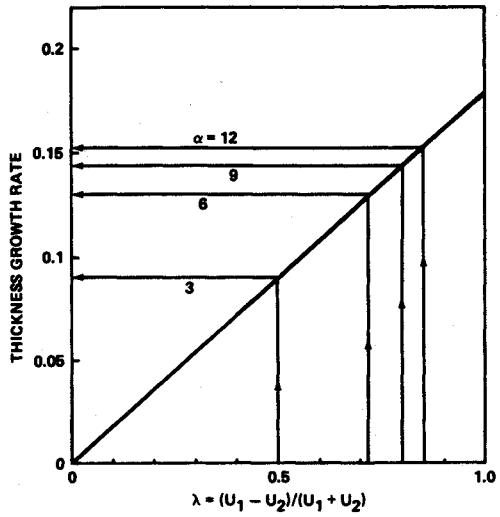

Fig. 12 Mixing layer growth rate as a function of the velocity difference parameter, $\lambda=(U_1-U_2)/(U_1+U_2)$.

The maximum return flow velocity in the CTRZ increases with increase in velocity ratio α (Fig. 13). It is seen that the maximum return flow velocity occurring on the centerline) is nearly proportional to the strength (U_a-U_p) of the mixing layer.

The characteristics of the corner recirculation zone are more complicated by the confining wall and the interaction of the two mixing layers. The variation of the length of the corner recirculation zone with velocity ratio is shown in Fig. 14. The increase in the length of the CRZ is gradual with the decrease of the velocity ratio up to 3. For $\alpha=2$, with no CTRZ, the length of the CRZ increases sharply. With a velocity ratio of unity, the flow resembles that of a simple pipe expansion flow and has a longer CRZ. The length is now 7.7 H, where H is the step height defined as $(D_e-D_0)/2$. For a simple pipe expansion of the same expansion ratio, the length of the CRZ was 8.7 H according to Moon and Rudinger.[20] The pipe wall extending beyond the expansion plane (see Fig. 9e) is responsible for the lower value of 7.7 H, as explained previously. With the tip ending at the expansion plane (Fig. 9c), the length of the CRZ is obtained as 8.5 H (shown in the figure by the point ⊙). It is instructive to note that Habib and Whitelaw[17] observe an increase in the length of the CRZ when the velocity ratio is increased from 1 to 3, in contrast to the present results. However, it should be noted that for $\alpha=3$, they do not observe any CTRZ in their geometry (expansion ratio of 2.81 and diameter ratio of 2.76). Johnson and Bennett[21] also do not find a CTRZ for $\alpha=3.11$ for their geometry (expansion ratio of 2.07 and diameter ratio of 1.93).

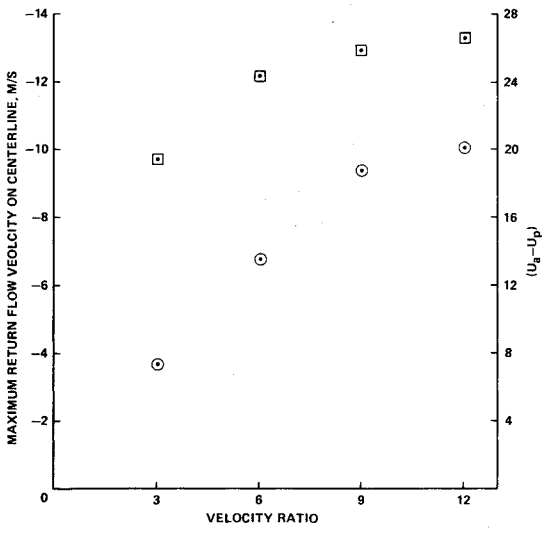

Fig. 13 Effect of velocity ratio on the maximum return flow velocity in the central toroidal recirculation zone [⊙ $-U_{max}$, ⊡ (U_a-U_p)].

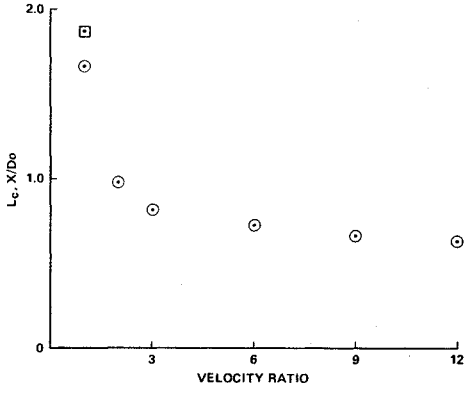

Fig. 14 Effect of velocity ratio on the length of the corner recirculation zone.

V. Conclusions

1) In a coaxial jet flow, the corner and central recirculation zones are very sensitive to the central jet exit geometry. The numerical solution can predict them reasonably accurately.

2) The velocity ratio determines the axial location of the central toroidal recirculation zone.

3) For the geometrical configuration studied, the length of the corner recirculation decreases with increase in velocity ratio, in contrast with the results of Habib and Whitelaw.[17]

4) For a velocity ratio of 3, the experimental configuration of Owen[7] results in the formation of the central toroidal recirculation zone, while the configurations of Habib and Whitelaw[17] and Johnson and Bennett[21] produce no CTRZ.

5) The k-ϵ turbulence model predicts the location, shape, and size of the recirculation zones fairly well. In these regions, the predicted axial and radial mean velocities and axial turbulence intensity are in good agreement with the measurements. However, the redevelopment of the flow beyond the reattachment on the centerline is slow compared to the measurements.

Acknowledgments

This work was supported by USRA Contract NAS8-35918, SSME Internal Flow Processes and was performed at the NASA Marshall Space Flight Center.

References

[1]Gupta, A. K., Lilley, D. G., and Syred, N., *Swirl Flows*, Abacus Press, London, 1984.

[2]Lefebvre, A. H., (ed.), *Gas Turbine Combustor Design Problems*, Hemisphere, New York, 1980.

[3]Jones, W. P. and Whitelaw, J. H., "Calculation Methods for Reacting Turbulent Flows: A Review," *Combustion and Flame*, Vol. 48, 1982, pp. 1-26.

[4]Nallasamy, M. and Hussain, A. K. M. F., "Numerical Study of the Phenomenon of Turbulence Suppression in a Plane Shear Layer," *Turbulent Shear Flows*, Vol. 4, 1984, pp. 169-181.

[5]Boyson, F., Ayers, W. H., Swithenbank, J., and Pan, Z., "Three Dimensional Model of Spray Combustion in Gas Turbine Combustors," *Journal of Energy*, Vol. 6, 1982, pp. 368-375.

[6]Swithenbank, J., Turan, A., and Felton, P. G., "Three Dimensional Two-Phase Mathematical Modeling of Gas Turbine Combustors," Project SQUID, Gas Turbine Combustor Design Problems, Purdue University, Lafayette, IN, 1978.

[7]Owen, F. K., "Measurement and Observations of Turbulent Recirculating Jet Flows," *AIAA Journal*, Vol. 14, 1976, pp. 1556-1562.

[8]Novick, A. S., Miles, G. A., and Lilley, D. G., "Numerical Simulation of Combustor Flow Fields: A Primitive Variable Design Capability," *Journal of Energy*, Vol. 3, 1979, pp. 95-105.

[9]Syed, S. A. and Sturgess, G. A., "Validation Studies of Turbulence and Combustion Models for Aircraft Gas Turbine Combustor," *Momentum and Heat Transfer Process in Recirculating Flow*, HTD Vol. 13, 1980, pp. 71-89.

[10]Sturgess, G. J., Syed, S. A., and McManus, K. R., "Importance of Inlet Boundary Conditions for Numerical Simulation of Combustor Flows," AIAA Paper 83-1263, 1983.

[11]Launder, B. E. and Spalding, D. B., "The Numerical Computation of Turbulent Flows," *Computational Methods in Applied Mechanics and Engineering*, Vol. 3, 1974, pp. 269-289.

[12]Nallasamy, M., "A Critical Evaluation of Various Turbulence Models as Applied to Internal Fluid Flows," NASA TP 2474, 1985.

[13]Spalding, D. B., "A General Purpose Computer Program for Multidimensional Two-Phase Flow," *Mathematics and Computers in Simulation*, Vol. XIII, 1981, pp. 267-276.

[14]Gossman, A. D. and Pun, W. M., "Calculation of Recirculating Flows," Dept. of Mechanical Engineering, Imperial College, London, Rept. GTS/74/12, 1974.

[15]Nallasamy, M. and Chen, C. P., "Studies on Effects of Boundary Conditions in Confined Turbulent Flow Predictions," NASA CR-3929, 1985.

[16]Habib, M. A. and Whitelaw, J. H., "Velocity Characteristics of a Confined Coaxial Jet," *Journal of Fluids Engineering*, Vol. 101, 1979, pp. 521-529.

[17]Habib, M. A. and Whitelaw, J. H., "Velocity Characteristics of Confined Coaxial Jets With and Without Swirl," *Journal of Fluids Engineering*, Vol. 102, 1980, pp. 47-53.

[18] Pope, S. B. and Whitelaw, J. H., "The Calculation of Near Wake Flows," *Journal of Fluid Mechanics*, Vol. 73, 1976, pp. 9-32.

[19]Brown, G. L. and Roshko, A., "On Density Effects and Large Structures in Turbulent Mixing Layers," *Journal of Fluid Mechanics*, Vol. 64, 1974, pp. 775-816.

[20]Moon, L.F. and Rudinger, G., "Velocity Distribution in an Abruptly Expanding Circular Duct," *Journal of Fluids Engineering*, Vol. 99, 1977, pp. 226-230.

[21]Johnson,, B.V. and Bennett, J. C., "Mass and Momentum Transport Experiments with Confined Coaxial Jets," NASA CR-165574, 1981.